Cell Reports, Volume *24*

Supplemental Information

PI3K-Mediated Blimp-1 Activation Controls B Cell Selection and Homeostasis

Corinna S. Setz, Eva Hug, Ahmad Khadour, Hend Abdelrasoul, Mayas Bilal, Elias Hobeika, and Hassan Jumaa

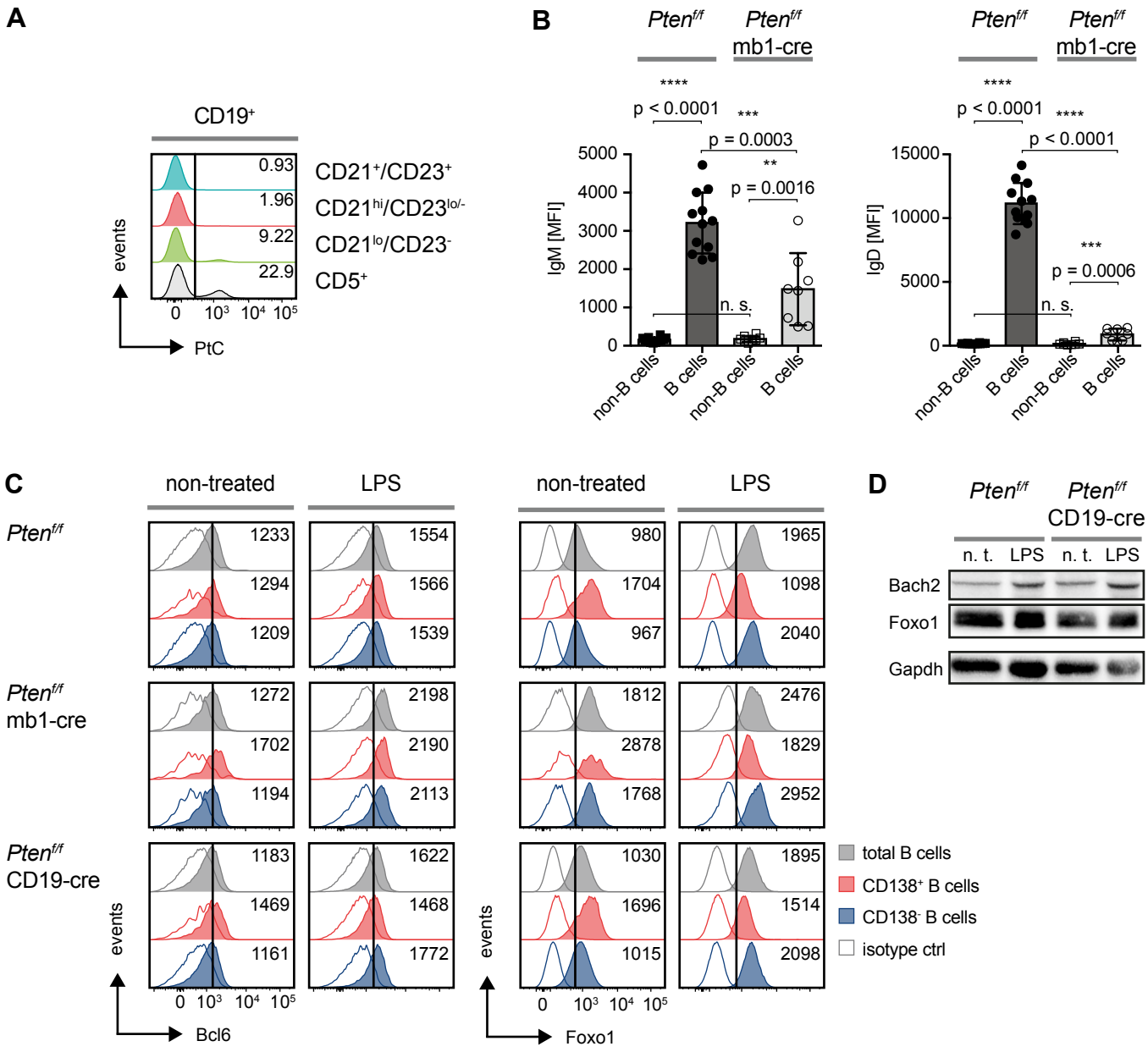

Figure S1 | Reduced BCR Expression in Pten-Deficient Mice and Analysis of Transcription Factors (related to Fig. 1 and 2)

A | Representative flow cytometric analysis of phosphatidylcholine (PtC)-binding in subpopulations of splenic B cells in control mice: Follicular B cells (Fo.B, CD21^{+}/CD23^{+}), marginal zone (MZ.B, CD21^{hi}/CD23$^{lo/-}$) and CD21^{lo}/CD23^{-} B cells.

B | Quantification of IgM (left) and IgD (right) mean fluorescence intensity (MFI) in splenic fractions of B cells and non-B cells from *Pten$^{f/f}$* (n=12) and *Pten$^{f/f}$* x mb1-cre mice (n=8) (mean ±SD). Average MFIs from 3 individual stainings per mouse were calculated. Statistical significance was calculated between B cells and non-B cells from the same mice by using the two-tailed paired t test, otherwise, by applying the two-tailed unpaired t test.

C | Intracellular flow cytometric analysis of Bcl6 (left) and Foxo1 (right) expression in splenocytes from Fig. 2A at day 3 following stimulation with 2.5 µg/ml LPS.

D | Immunoblot analysis of Bach2 and Foxo1 expression in splenocytes from Fig. 2A at day 3. n. t. = non-treated, Gapdh served as loading control. Data are representative of at least 2 mice per genotype.

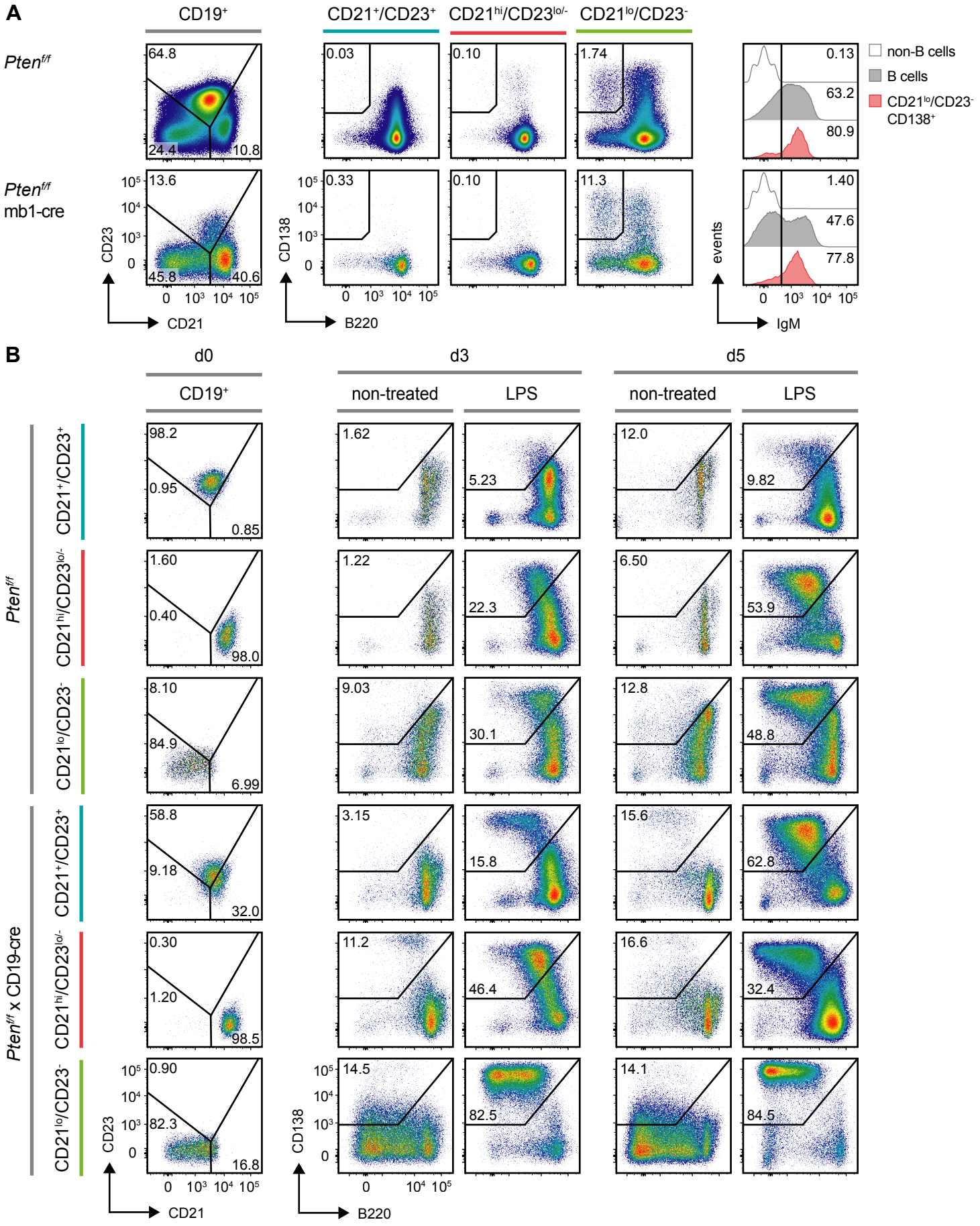

Figure S2 | B Cells From Pten-Deficient Mice are Committed to Terminal Differentiation (related to Fig. 2)

A | Representative staining of CD19^{+}/B220^{lo}/CD138^{+} plasma cells in Fo.B (CD21^{+}/CD23^{+}), MZ.B (CD21^{hi}/CD23$^{lo/-}$) and CD21^{lo}/CD23^{-} splenic B cell subpopulations from *Pten*$^{f/f}$ and *Pten*$^{f/f}$ x mb1-cre mice. CD19^{+}/B220^{lo}/CD138^{+} cells in CD21^{lo}/CD23^{-} B cells were further analyzed for surface IgM expression. Data are representative of at minimum 2 mice per genotype.

B | Fo.B (CD21^{+}/CD23^{+}), MZ.B (CD21^{hi}/CD23$^{lo/-}$) and CD21^{lo}/CD23^{-} splenic B cell populations were FACS-purified from spleens of *Pten*$^{f/f}$ and *Pten*$^{f/f}$ x CD19-cre mice. Cells were either left untreated or cultured in presence of LPS (2.5 µg/ml) for 5 days and surface expression of CD138 and B220 was assessed at the indicated time points. Data are representative of at least 3 mice per genotype.

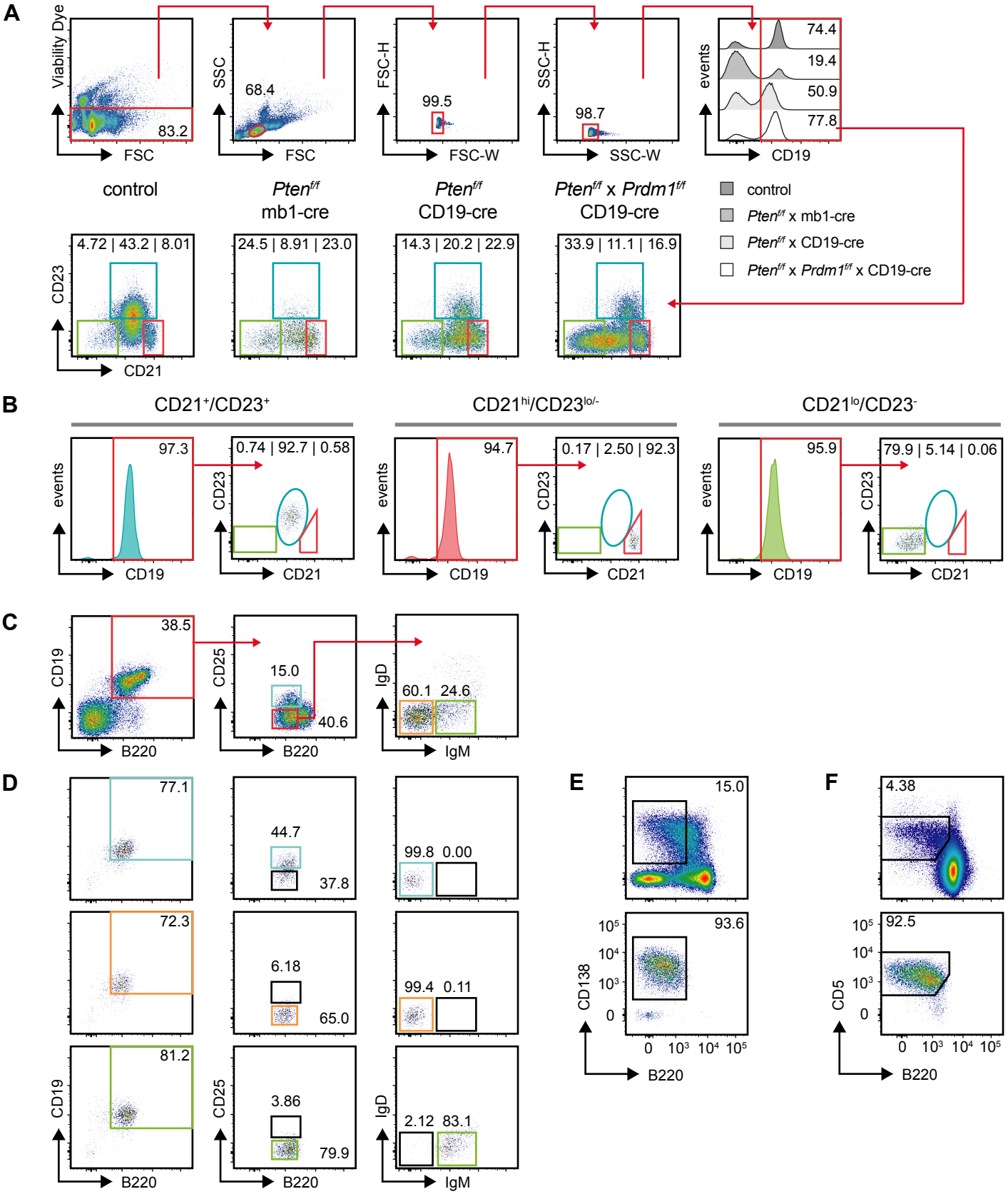

Figure S3 | Increased Blimp-1 Expression in Pten-Deficient B Cells (related to Fig. 2 and 4)

A | Fo.B ($CD21^+/CD23^+$, blue), MZ.B ($CD21^{hi}/CD23^{lo/-}$, red) and $CD21^{lo}/CD23^-$ B cells (green), from spleens of control, *Pten*$^{f/f}$ x mb1-cre, *Pten*$^{f/f}$ x CD19-cre and *Pten*$^{f/f}$ x *Prdm1*$^{f/f}$ x CD19-cre mice were FACS-purified as illustrated by the gating strategy.

B | Representative re-analysis of splenic B cell populations from the control mouse, purified according to the gating strategy shown in Fig. S3A to determine the purity of the sorted populations.

C | Pro-B cells ($CD19^+/B220^+/IgM^-/IgD^-/CD25^-$, orange), small pre-B cells ($CD19^+/B220^+/IgM^-/IgD^-/CD25^+$, blue) and immature B cells ($CD19^+/B220^+/IgM^+/IgD^-/CD25^-$, green) from control mice were FACS-purified as illustrated by the gating strategy.

D | Representative re-analysis of B cell populations purified according to the gating strategy shown in Fig. S3C to determine the purity of the sorted populations.

E | Splenocytes from wild-type mice were stimulated with 2.5 μg/ml LPS for 5 days. $B220^{lo}/CD138^+$ were FACS-purified (top) and subsequently re-analyzed to assess the purity (bottom).

F | Splenic B-1a B cells from wild-type mice (pre-gated on $CD19^+$ cells) were FACS-purified (top) and re-analyzed subsequently to assess the purity (bottom).

Dead cells and doublets were removed also during purification of populations in Fig. S3C, E and F as shown in Fig. S3A.

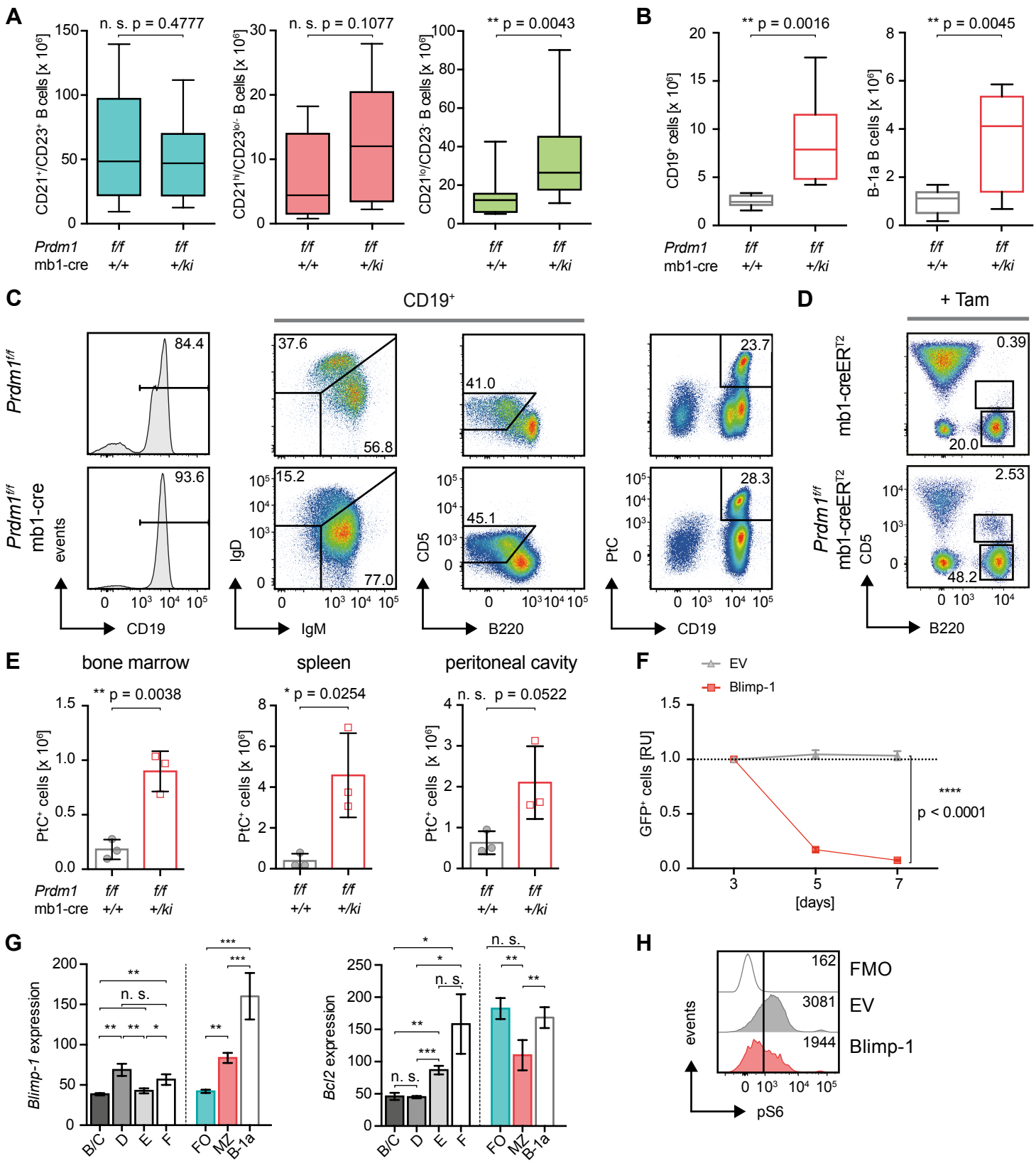

Figure S4 | Increased Autoreactivity in *Prdm1*-Deficient B Cells (related to Fig. 3 and 4)

A | Cell numbers of splenic Fo.B (blue), MZ.B (red) and CD21^{lo}/CD23^{-} (green) B cells from *Prdm1$^{f/f}$* and *Prdm1$^{f/f}$* x mb1-cre mice (n=14, median ±quartile and range).

B | Absolute numbers of total B cells and B-1a B cells in peritoneal cavities from *Prdm1$^{f/f}$* and *Prdm1$^{f/f}$* x mb1-cre mice (n=8, median ±quartile and range).

C | Representative flow cytometric analyses of peritoneal cavity lavages from *Prdm1$^{f/f}$* and *Prdm1$^{f/f}$* x mb1-cre mice for surface expression of the indicated markers and binding of phosphatidylcholine (PtC).

D | Representative flow cytometric analysis of peripheral blood cells from mice of the indicated genotypes 6 months after inducible deletion of *Prdm1* by tamoxifen (+ Tam) administration (bottom). Mice expressing mb1-cre-ER^{T2} in absence of floxed alleles (top) treated with tamoxifen served as control. Shown data are representative for at least 2 individual mice per genotype.

E | Numbers of PtC-reactive B cells in bone marrow, spleens and peritoneal cavities from mice of the indicated genotypes (n=3, mean ±SD).

F | Survival of *Rag2/λ5* double knock-out (DKO) pro-B cells upon ectopic overexpression of Blimp-1 or the empty vector (EV). Percentages of viable GFP^{+} cells at days 5 and 7 were normalized to the percentages measured at day 3 after transduction (n=6, mean ±SD).

G | Analysis of published microarray data on gene expression of *Blimp-1* (left) and *Bcl2* (right) in Hardy fractions B/C (pro), D (pre), E (newly formed) and F (recirculating B cells) compared to expression in Fo.B, MZ.B and B1-a B cells of the murine spleen (n=3 ±SD).

H | Measurement of mTor activity by pS6 content via FACS in *Rag2/λ5* DKO pro-B cells at day 3 upon retroviral transduction with an expression vector encoding Blimp-1 or the EV, respectively. Untransduced cells unstained for pS6 (FMO, fluorescence minus one) served as control.

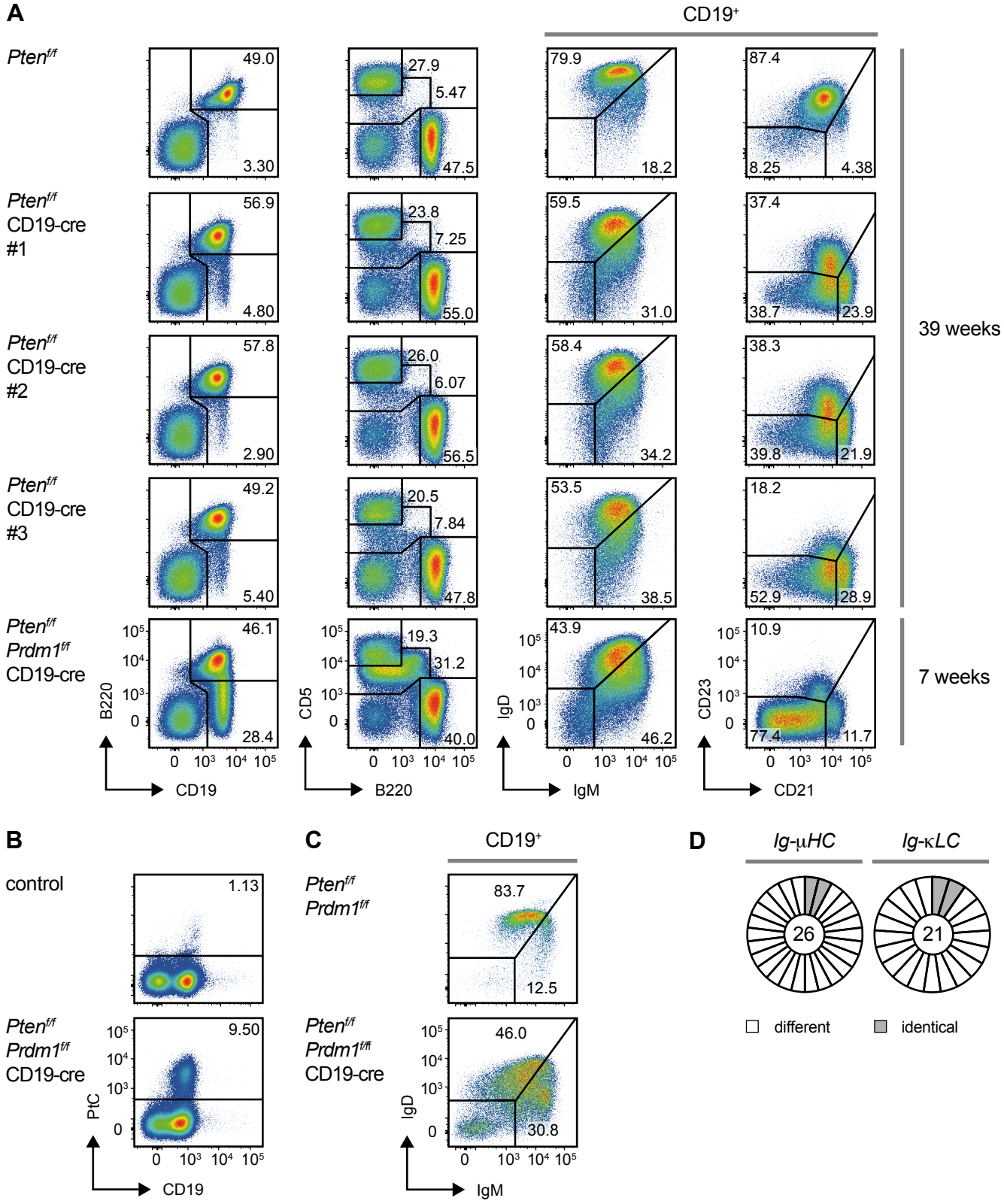

Figure S5 | Premature Terminal Differentiation Prevents Uncontrolled Proliferation (related to Fig. 5)

A | Splenic B cell subpopulations from *Pten*$^{f/f}$, *Pten*$^{f/f}$ x CD19-cre (both sacrificed at the age of 39 weeks) and *Pten*$^{f/f}$ x *Prdm1*$^{f/f}$ x CD19-cre (7 weeks) were compared by flow cytometry.

B | Splenocytes from control and *Pten*$^{f/f}$ x *Prdm1*$^{f/f}$ x CD19-cre mice were analyzed by flow cytometry for surface expression of CD19 and reactivity to phosphatidylcholine (PtC).

C | Peripheral blood from *Pten*$^{f/f}$ x *Prdm1*$^{f/f}$ and *Pten*$^{f/f}$ x *Prdm1*$^{f/f}$ x CD19-cre mice was analyzed by flow cytometry for BCR expression (IgM/IgD).

D | Analysis of V(D)J gene segment usage in CD19^{+}/CD5^{+} B cells from *Pten*$^{f/f}$ x *Prdm1*$^{f/f}$ x CD19-cre mice (n=2). The V(D)J segments from *Ig*-μ*HC* and *Ig*-κ*LC* were cloned from cDNA, sequenced and the frequency of identical combinations was analyzed to assess the BCR clonality of the respective cells in these mice. For further details see also Table S7.

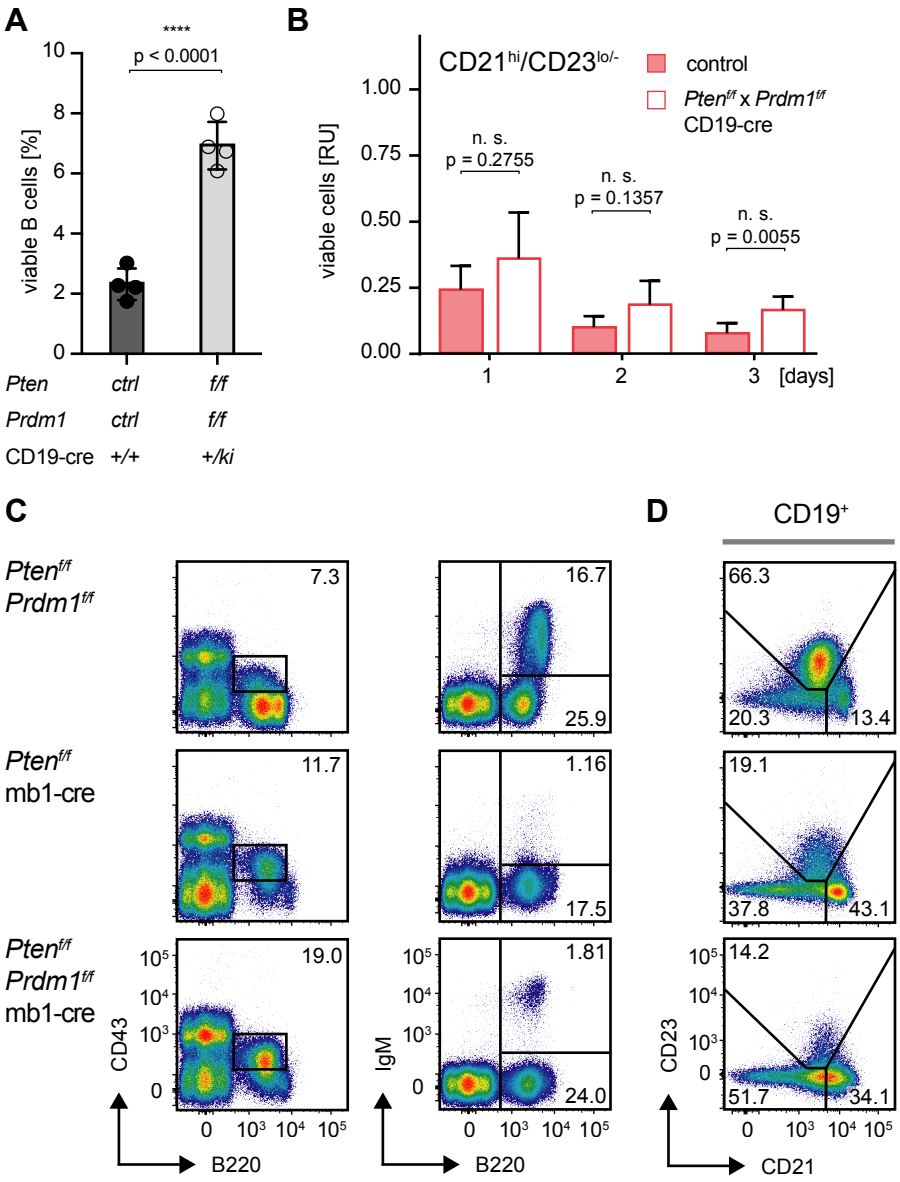

Figure S6 | Reconstitution of Blimp-1 Activates Terminal Differentiation
(related to Fig. 6)

A | Splenocytes from control and *Pten*$^{f/f}$ x *Prdm1*$^{f/f}$ x CD19-cre mice were treated with 2.5 µg/ml LPS. The percentages of viable cells were assessed at 7 days post stimulation by morphology and staining with viability dye, α-CD19 and α-B220 (n=4, mean ±SD).

B | MZ.B cells (CD21^{hi}/CD23$^{lo/-}$) from mice of the indicated genotypes were FACS-purified and cultured *in vitro*. The percentages of viable cells were monitored over a time period of 3 days and assessed by morphology and staining with viability dye. Percentages of viable cells at each timepont were normalized to the percentages of viable cells measured at day 0 in the respective sample (n=4, mean, +SD).

C, D | Freshly isolated bone marrow (**C**) and splenocytes (**D**) from *Pten*$^{f/f}$ x *Prdm1*$^{f/f}$ and *Pten*$^{f/f}$ x *Prdm1*$^{f/f}$ x mb1-cre mice were analyzed by flow cytometry for surface expression of the indicated markers. Data are representative of 2 individual mice sacrificed and analyzed at the age of 10 and 17 weeks, respectively.

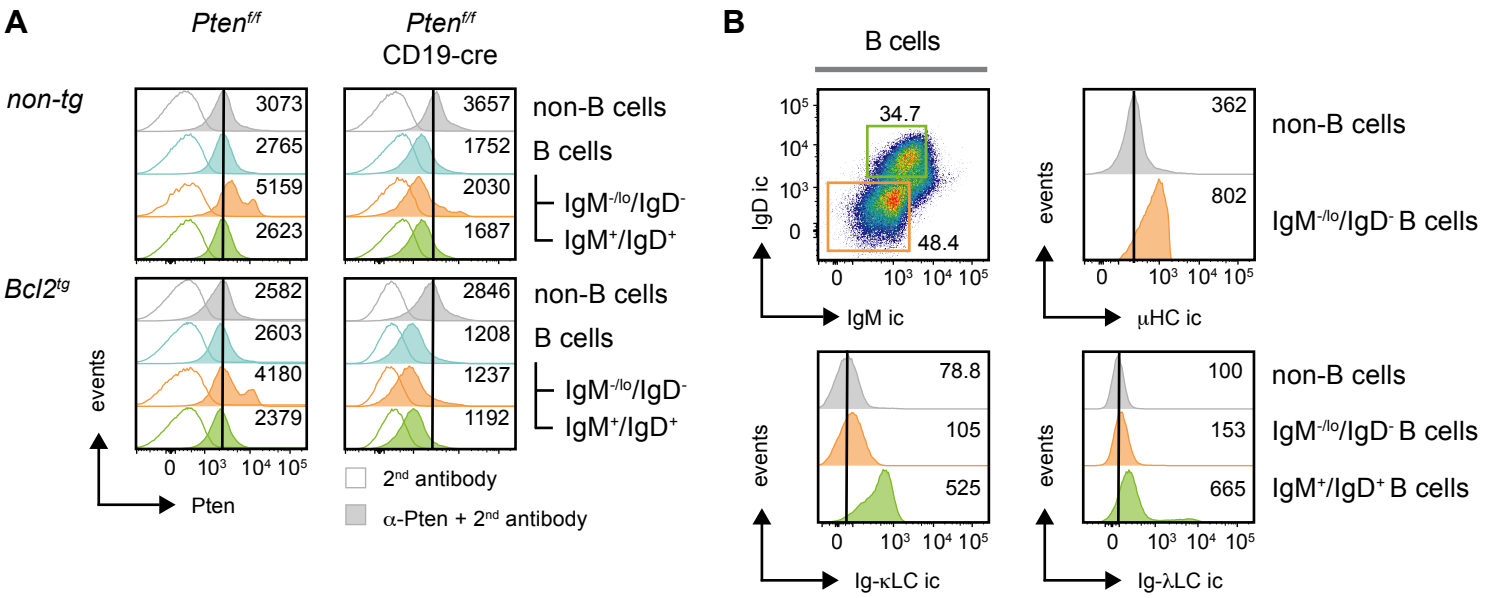

Figure S7 | Characterization of the IgM$^{-/lo}$/IgD^{-} Population in *Pten$^{f/f}$* x CD19-cre x *Bcl2^{tg}* Mice (related to Fig. 7)

A | Splenocytes from mice of the indicated genotypes were stained intracellularly for Pten following surface staining for CD19, B220, IgM and IgD. Pten deletion was compared in the populations of non-B cells (CD19^{-}/B220^{-}), total B cells (CD19^{+}/B220^{+}), BCR^{+} (CD19^{+}/B220^{+}/IgM^{+}/IgD^{+}) and BCR$^{-/lo}$ (CD19^{+}/B220^{+}/IgM$^{-/lo}$/IgD^{-}) B cells.

B | *Pten$^{f/f}$* x CD19-cre x *Bcl2^{tg}*-derived splenocytes were stained at the surface for expression of CD19 and B220, subsequently fixed, permeabilized and stained intracellularly (ic) for IgM, IgD, Ig-κ- and Ig-λLC. Intracellular Ig-μHC expression in the IgM$^{-/lo}$/IgD^{-} population was compared to expression in the non-B cell fraction (CD19^{-}/B220^{-}). Intracellular Ig-κ- and Ig-λLC expression in the IgM$^{-/lo}$/IgD^{-} population was compared to the expression in the IgM^{+}/IgD^{+} B cell and the non-B cell fraction (CD19^{-}/B220^{-}).

Supplemental Experimental Procedures

Tamoxifen Administration

For inducible deletion of *Prdm1*, *Prdm1*$^{f/f}$ mice were intercrossed with mb1-cre-ER^{T2} mice (Hobeika et al., 2015) and treated by gavage 3x every second day with 6 mg tamoxifen (Ratiopharm) dissolved in 20% ClinOleic (Baxter). Inducible deletion of *Prdm1 in vivo* was performed in compliance with animal research permit #1288 at the regional board of Tübingen, Germany). Mice were sacrificed and analyzed 6 months after induction with tamoxifen.

Table S1 | Antibodies used in flow cytometric analyses (related to Experimental Procedures)

Antigen	Conjugate	Clone	Company
CD5	eFluor 450 or PE	53-7.3	eBioscience
CD19	PerCP-Cy5.5	1D3	BD Biosciences
CD19	eFluor 450 or APC	eBio1D3	eBioscience
CD21/CD35	APC or PE-Cy7	7E9	BioLegend
CD23	PE or Biotin	B3B4	BD Biosciences
CD25	APC	PC61	BD Biosciences
CD43	FITC	S7	BD Biosciences
CD45R (B220)	PE-Cy7 or PerCP-eFluor 710	RA3-642	eBioscience
CD138	PE	DL-101	eBioscience
CD138	Brilliant Violet 421	281-2	BioLegend
IgD	FITC, PE or Biotin	11-26	SouthernBiotech
IgD	APC	11-26	eBioscience
IgM	FITC	polyclonal	SouthernBiotech
IgM	eFluor 450	eB121-15-F9	eBioscience
IgM	Cy5	polyclonal	Jackson Immunoresearch
Bcl2	PE	Bcl-2/100	BD Biosciences

Bcl6	Alexa Fluor 647	K112-91	BD Biosciences
Blimp-1	Alexa Fluor 647	5E7	BioLegend
Irf4	eFluor 660	3E4	eBioscience
pS6	PE or PerCP-eFluor710	cupk43k	eBioscience
Pten	unlabeled	138G6	Cell Signaling
Foxo1	unlabeled	C29H4	Cell Signaling
Isotype ctrl.	Alexa Fluor 647 or PE	MOPC-173 and MOPC-21	BioLegend
Isotype ctrl.	eFluor 660	eB149/10H5	eBioscience

Table S2 | Fixation and permeabilization kits used for intracellular flow cytometry (related to Experimental Procedures)

Antigen	Kit	Company
Bcl2, Foxo1, Pten and BCR	Fix and perm cell permeabilization kit	ADG
Bcl6	Foxp3 Staining Buffer Set	eBioscience
Blimp-1 and Irf4	True-Nuclear Transcription Buffer Staining Set	BioLegend
pS6	Cytofix/Cytoperm Kit	BD Biosciences

Table S3 | Antibodies used for immunoblotting (related to Experimental Procedures)

Antigen	origin	Clone	Company
Blimp-1	rabbit	C14A1	Cell Signaling
Bach2	rabbit	polyclonal	Rockland
Irf4	rabbit		abcam
Irf8	rabbit	D20D8	Cell Signaling
Foxo1	rabbit	C29H4	Cell Signaling
pS6	rabbit	D57.2.2E	Cell Signaling
Gapdh	rabbit	D16H11	Cell Signaling

Table S4 | Antibodies used for immunohistochemistry (related to Experimental Procedures)

Antigen	Conjugate	Clone	Company
CD169	FITC	MOMA-1	AbD serotec
CD90.2	PE	53-2.1	BD Biosciences
IgM	Cy5	polyclonal	Jackson Immunoresearch

Table S5 | TaqMan-Probe mixes used for qPCR analyses

(related to Experimental Procedures)

TaqMan-Probe mixes	
Prdm1	Mm00476128_m1
Bcl2	Mm00477631_m1
Gapdh	Mm99999915_g1

RACE

Total RNA was isolated from sorted cells and cDNA was synthesized as described in the main experimental procedures section concerning quantitative RT-PCR. A poly G-tail was added to the 3' end of the first strand cDNA using dGTP and TdT (New England Biolabs). *Ig-μHC*-specific and *Ig-κLC*-specific transcripts were amplified by nested PCR using gene-specific oligos, anchor/adaptor oligos (enlisted in Table S6) and Q5 polymerase (New England Biolabs). The amplified PCR-products were subcloned in pJET1.2 blunt/vector (CloneJET PCR Cloning Kit, Thermo Fisher) and colonies were sequenced (GATC). Sequences were analyzed by using the ImMunoGeneTics information system IMGT/V-Quest online tool.

Table S6 | Primers used for *Ig* gene RACE (related to Experimental Procedures)

Ig-μHC amplification

Primers 1st PCR		Sequence 5'→ 3'
BaPpc	Anchor	CTC TGC AGG ATC CAC GAC CCC CCC CCC CCC C
mmuSP2		GAC CAG ACA GGT CAG GTT AGC GGA CTT GCT

Primers 2nd PCR		Sequence 5'→ 3'
BaP	Adaptor	TCT GCA GGA TCC ACG ACC
mmuSP3		GAT GAC TTC AGT GTT GTT CTG GTA GTT CCA

Ig-κHC amplification

Primers 1st PCR		Sequence 5'→ 3'
BaPpc	Anchor	CTC TGC AGG ATC CAC GAC CCC CCC CCC CCC C
mK-SP2		TGA AGT TGA TGT CTT GTG AGT GGC CTC

Primers 2nd PCR		Sequence 5'→ 3'
BaP	Adaptor	TCT GCA GGA TCC ACG ACC
mK-SP1		TCA AGA AGC ACA CGA CTG AGG

Table S7 | *Ig* gene RACE sequencing results (related to Fig. 5 and Fig. S5D)

Ig-μHC

# 5462 DKO CD19⁺ CD5⁺					
Clone N.	V-GENE and allele	J-GENE and allele	D-GENE and allele	HCDR3	Length
C 16	IGHV1-12*01 F	IGHJ2*01 F	IGHD2-3*01 F	CARDVHFDYW	8
C 17	IGHV1-59*01 F	IGHJ3*01 F	IGHD2-3*01 F	CAREGDGYAYW	9
C 21	IGHV5-17*01 F	IGHJ4*01 F	IGHD2-14*01 F	CARQYRAMDYW	9
C 22	IGHV5-17*01 F	IGHJ4*01 F	IGHD2-14*01 F	CARPRYHTMDYW	10
C 23	IGHV1-72*01 F	IGHJ2*01 F	IGHD2-10*02 F	CAYGNYVYYFDYW	11
C 24	IGHV1-77*01 F	IGHJ3*01 F	IGHD2-2*01 F	CARGGGYVLFAYW	11
C 25	IGHV11-2*01 F	IGHJ1*03 F	IGHD1-1*01 F	CMRYGSSYWYFDVW	12
C 26	IGHV9-3*01 F	IGHJ3*01 F	IGHD2-3*01 F	CARPDGYLFAYW	10
C 27	IGHV1-75*01 F	IGHJ3*01 F	IGHD3-3*01 F	CARGGTGFAYW	9
C 28	IGHV6-6*01 F	IGHJ2*01 F	IGHD1-1*01 F	CTRHYGSSYYFDYW	12
C 29	IGHV9-4*01 F	IGHJ3*01 F	IGHD1-1*01 F	CARSYYYGSSYSWFAYW	15
C 30	IGHV1-50*01 F	IGHJ2*01 F	IGHD1-1*02 F	CARGDYFDYW	8

# 5464 DKO CD19⁺ CD5⁺					
	V-GENE and allele	J-GENE and allele	D-GENE and allele	HCDR3	Length
C 44	IGHV5-9-1*02 F	IGHJ4*01 F	IGHD2-3*01 F	CTRDDDGYFYYYAMDYW	15
C 45	IGHV8-8*01 F	IGHJ2*01 F	IGHD2-10*01 F	CARTPYYGRGFDYW	12
C 46	IGHV9-3*01 F	IGHJ4*01 F	IGHD2-2*01 F	CARTTTDTAMDYW	11
C 47	IGHV1-19*01 F	IGHJ1*03 F	IGHD2-1*01 F	CARVYGNWYFDVW	11
C 48	IGHV9-3*01 F	IGHJ2*01 F	IGHD3-3*01 F	CARIGGLYYFDYW	11
C 49	IGHV2-9-1*01 F	IGHJ3*01 F	IGHD2-2*01 F	CARYGYDGGPWFAYW	13
C 50	IGHV1-19*01 F	IGHJ3*01 F	IGHD1-1*02 F	CGGGNYGWFAYW	10
C 51	IGHV1-63*01 F	IGHJ3*01 F	IGHD3-1*01 F	CARGLTWFAYW	9
C 52	IGHV5-6*01 F	IGHJ1*03 F	IGHD2-4*01 F	CARPLYDYDYWYFDVW	14
C 53	IGHV1-55*01 F	IGHJ2*01 F	no	CARRDYW	5
C 54	IGHV5-17*01 F	IGHJ1*03 F	IGHD2-3*01 F	CARCYYRYFDVW	10
C 55	IGHV1-19*01 F	IGHJ2*01 F	IGHD2-4*01 F	CARGLDYDGGYW	10
C 56	IGHV11-2*01 F	IGHJ1*03 F	IGHD2-1*01 F	CMRYGNYWYFDVW	11
C 57	IGHV9-3*01 F	IGHJ2*01 F (a)	IGHD6-3*01 F	CARDSTVDYW	8

Ig-κLC

# 5462 DKO CD19⁺ CD5⁺				
Clone N.	V-GENE and allele	J-GENE and allele	LCDR3	Length
C 2	IGKV8-27*01 F	IGKJ5*01 F	CHQYLSSLTF	8
C 10	IGKV3-10*01 F	IGKJ2*01 F	CQQNNEDPYTF	9
C 11	IGKV8-16*01 F	IGKJ2*01 F	CQQHLHIPYTF	9
C 12	IGKV17-121*01 F	IGKJ5*01 F	CLQSDNLPLTF	9
C 14	IGKV14-126*01 F	IGKJ4*01 F	CLQHGESPFTF	9
C 19	IGKV14-126*01 F	IGKJ1*01 F	CLQHGESPWTF	9
C 26	IGKV12-44*01 F	IGKJ2*01 F	CQHHYGTPYTF	9
C 29	IGKV4-91*01 F	IGKJ5*01 F	CQQGSSIPLTF	9
C 31	IGKV8-16*01 F	IGKJ4*01 F	CQQHLHIPYTF	9

# 5464 DKO CD19⁺ CD5⁺				
	V-GENE and allele	J-GENE and allele	LCDR3	Length
C 3	IGKV5-39*01 F	IGKJ5*01 F	CQNGHSFPLTF	9
C 5	IGKV8-24*01 F	IGKJ1*01 F	CQQHYSTPRTF	9
C 6	IGKV4-91*01 F	IGKJ5*01 F	CQQGSSIPLTF	9
C 7	IGKV5-39*01 F	IGKJ4*01 F	CQNGHSFPFTF	9
C 9	IGKV4-59*01 F	IGKJ2*01 F	CQQWSSYPYTF	9
C 12	IGKV5-39*01 F	IGKJ2*01 F	CQNGHSFPYTF	9
C 16	IGKV14-126*01 F	IGKJ2*01 F	CLQHGESPYTF	9
C 19	IGKV12-44*01 F	IGKJ2*01 F	CQHHYGTPYTF	9
C 20	IGKV8-21*01 F	IGKJ1*01 F	CKQSYNLPWTF	9
C 23	IGKV5-39*01 F	IGKJ2*01 F	CQNGHSFPYTF	9
C 25	IGKV8-21*01 F	IGKJ1*01 F	CKQSYNLPWTF	9
C 27	IGKV19-93*01 F	IGKJ1*01 F	CLQYDNLWTF	8

Identical V(D)J segments are marked in grey

Supplemental references

Hobeika, E., Levit-Zerdoun, E., Anastasopoulou, V., Pohlmeyer, R., Altmeier, S., Alsadeq, A., Dobenecker, M.W., Pelanda, R., and Reth, M. (2015). CD19 and BAFF-R can signal to promote B-cell survival in the absence of Syk. EMBO J *34*, 925-939.